On the possible structural role of single chain sphingolipids Sphingosine and Sphingosine 1-phosphate in the amyloid-β peptide interactions with membranes. Consequences for Alzheimer's disease development

Chiho Watanabe, Michel Seigneuret, Galya Staneva, Nicolas Puff, Miglena Angelova

On the possible structural role of single chain sphingolipids Sphingosine and Sphingosine 1-phosphate in the amyloid-β peptide interactions with membranes. Consequences for Alzheimer's disease development.

Chiho Watanabe[a], Michel Seigneuret[a], Galya Staneva[b], Nicolas Puff[a,c*] and Miglena I. Angelova[a,c*]

[a] *Laboratoire Matière et Systèmes Complexes, (MSC) CNRS UMR 7057, Univ. Paris Diderot-Paris 7, F3, Paris, France*

[b] *Institute of Biophysics and Biomedical Engineering, Bulgarian Academy of Sciences, Sofia, Bulgaria.*

[c] *Physics Department, UPMC-Univ. Paris 6, UFR 925, F5, Paris, France*

*Correspondence: to Miglena I. Angelova or Nicolas Puff , Matière et Systèmes Complexes, UMR 7057, Université Paris 7 Diderot & CNRS, 10 rue Alice Domon et Léonie Duquet 75205 Paris cedex 13, France; E-mail: miglena.anguelova@upmc.fr; nicolas.puff@univ-paris-diderot.fr, Tel: 33, (0)157277082; Fax: 33, (0)157276211

Statistics: 7285 words

8 figures

1 table

ABSTRACT: A strong interplay between the neurodegerative effects of the amyloid β, (Aβ) peptides and the cell lipid composition or metabolism has been evidenced in Alzheimer's disease. This appears to be, in part, related to Aβ-membrane interactions. Recently, an influence of the two cell fate-modulating single-chain sphingolipids sphingosine, (Sph) and sphingosine 1-phosphate, (S1P) on AD-related mechanisms has been reported. We have investigated the influence of Sph and S1P on the interaction of Aβ(1-42) with lipid model

membranes. A fluorescent Aβ(1-42) binds to egg phosphatidylcholine, (EPC) giant unilamellar vesicles containing Sph or S1P. With Sph, gel microdomains are present at low temperature and Aβ(1-42) binds preferentially to these domains, especially at their boundaries. With S1P, which displays single lipid phase morphology, Aβ(1-42) binding is uniform. The binding of Aβ(1-42) to EPC/sphingolipid large unilamellar vesicles was investigated by spectrofluorimetry using the 2 probes Laurdan and di-ANEPPS. With most lipid compositions the binding of Aβ(1-42) to LUVs appears superficial. However, with Sph, a deeper membrane penetration is observed. This deeper interaction is reversed to superficial by the simultaneous presence of S1P. It is suggested that the influence of single-chain sphingolipids in AD might be related to a selective interaction of Aβ(1-42) with sphingosine in membranes, that is antagonized by S1P. Such interaction might occur intracellularly for Aβ(1-42) monomers or oligomers and/or extracellularly for Aβ still part of APP. Aβ(1-42) might also influence microdomains by binding to their boundaries. The influence of the Sph/S1P balance on the Alzheimer pathology might be related in part to the differential interactions of Aβ(1–42) with Sph and S1P and their effects on membrane domains.

Keywords: *Alzheimer's disease,, Sphingosine, Sphingosine 1-phosphate, Amyloid beta-Peptide, Membrane Microdomains, Membrane dipole potential, Laurdan.*

INTRODUCTION

Alzheimer disease, (AD) is a degenerative disease of the central nervous system, which causes irreversible damage to neurons structure and function. Central to AD is the altered proteolytic processing on the Amyloid Precursor Protein, (APP) resulting in the enhanced production and the aggregation of Amyloid β peptide, (Aβ) with Aβ(1-42) and

Aβ(1) being its principal forms [1]. The most documented effect of Aβ occurs extracellularly though extensive Aβ aggregation, which according to the amyloid cascade hypothesis, leads to senile plaques formation [1]. However, despite a clear association between the build-up of the Aβ peptide(s) and cognitive decline in Alzheimer disease, a correlation between plaque deposition and the severity of dementia, has not been established. Cognitive decline appears to be correlated by defects in synaptic plasticity or function that precedes Aβ deposition [4]. Small soluble, non-fibrillar Aβ oligomers, which are also toxic [5] may be responsible for such early synaptic changes [6]. In this regard, several studies have suggested the occurrence of cytosolic amyloid-β peptide produced by different possible mechanisms [7].

Over these last years, studies on AD animal models, on cellular systems and on model systems have shown an amazing interplay between numerous aspects of AD and lipid composition and metabolism [12,13]. This has even led to the hypothesis that the non-pathological role of Aβ and its parent protein might be that of regulators of lipid homeostasis [14]. It appears likely that the role of specific lipids in the development of AD is at least in part related to Aβ/biomembrane interactions. Indeed the Aβ peptide contains both clusters of hydrophobic residues and charged sidechains that make it prone to bilayer insertion as well as to binding to specific lipid headgroups. Specific membrane lipids appear to be involved in the Aβ oligomerization and fibrillation process leading to plaque formation. In vivo correlations have been found between metabolism and content of cholesterol and gangliosides and AD-associated manifestations [15]. A complex between the ganglioside GM1 and Aβ has been reported to accumulate in AD brain tissue [16]. Numerous experiments with model membrane have shown that GM1 and cholesterol, separately and together, affect Aβ binding to bilayers, conformation and oligomerization [17,18]. Lipid rafts, which are membrane microdomains

enriched in cholesterol and sphingolipids, have been proposed to act as surface catalysts able to accelerate the aggregation of Aβ [19]. Thus such lipids may be involved in the extracellular processes that lead from production of extracellular Aβ to plaque formation.

Very recently, other types of lipids have been linked to AD. Among these, are the two bioactive signaling lipids sphingosine, (Sph) and sphingosine 1-phosphate, (S1P) [20]. Sph and S1P are single-chained charged sphingolipids that have antagonistic functions in the "sphingolipid rheostat" which determines cell fate [22]. Sph and S1P respectively promote apoptosis and cell growth. The interconversion between Sph and S1P involves specific intracellular kinases and phosphatases tightly regulated by stress or growth effectors. The antagonistic biological activities of both sphingolipids have been correlated with their direct targeting of enzymes, cofactors or receptors involved in apoptotic and proliferation pathways, but also with their direct effect on physicochemical properties of the lipid bilayer [25, 26]. An abnormal metabolism of both sphingolipids has been reported in Alzheimer's disease, (AD). More Sph was found in the AD brains, whereas S1P levels were reduced [27]. A decreased expression of Sph kinase 1 and an increased expression of sphingosine-phosphate lyase both correlated to amyloid deposits in the brain have been reported as well as a loss of S1P and sphingosine kinase activity early in AD pathogenesis, and prior to AD diagnosis [28, 29]. Sph and S1P appear to also interfere with the proteolytic release of Aβ [30, 31]. It is not known whether the perturbation of single chain sphingolipids metabolism levels is a cause or an effect of the development of AD associated processes. Since both sphingolipids are mainly produced intracellularly, (although also occurring extracellularly), an interplay between them and intracellular Aβ appears possible.

In the present study, we have addressed the possibility that Sph and S1P might have a structural role and affect Aβ(1–42) membrane binding. For this purpose we have studied the

binding of Aβ(1−42) to giant unilamellar vesicles, (GUVs) and large unilamellar vesicles, (LUVs) containing Sph and S1P. For GUVs binding both a fluorescently labeled Aβ(1-42), (Hilyte Fluor 488) and a lipid microdomain-sensitive membrane probe Texas Red PE were used. For LUVs, Aβ(1-42) binding was monitored through its effect on the spectroscopic properties of 2 different membrane-embedded fluorescence probes Laurdan and di-8-ANEPPS which report on distinct membrane properties. Laurdan reports on the orientational polarizability of its membrane environment, mainly of water molecules. Such orientational polarizability depends on the polarity of the environment as well as its fluidity [32]. Since changes in lipid packing affect the access of water into the membrane (and therefore the polarity) as well as the freedom of motion, (i.e. the fluidity), Laurdan is commonly used as a probe of lipid packing [33]. di-8-ANEPPS reports on membrane dipole potential. The dipole potential is the electrical potential that occurs transversally between the water-lipid interface and the hydrocarbon interior. It depends on the nature of the membrane dipoles (lipid groups, water) and how tightly packed these dipoles are [34]. di-8-ANEPPS measurements of dipole potential can be made independant of fluidity by appropriate choice of the detection wavelength [35]. It has recently been put forward that the dipole potential has a strong effect on the activity of membrane proteins and on the membrane binding of peptides [36, 37]. Besides, the measurement of dipole potential reports upon the mode of peptide membrane binding [38].

MATERIALS & METHODS

Chemicals.

Egg yolk L-α- phosphatidylcholine, (EPC), D-*erythro*-Sphingosine, (Sph) and D-*erythro*-sphingosine-phosphate, (S1P) were from Avanti Polar Lipids, (Alabaster, AL). Di-ANEPPS and Texas Red DPPE, (TR-PE) were from Invitrogen, Carlsbad, CA. Laurdan was from Molecular Probes, (Waltham, MS). Lipid stock solutions were prepared as described previously [25].

Aβ(1-42) sample preparation

Aβ(1-42), (Bachem) was suspended in hexafluoroisopropanol to a concentration of 0.57 mg/mL, sonicated at 50˚C for 1h, aliquoted, dried under argon and held under vacuum for 2 hours. Before use, dried Aβ(1-42)was solubilized by addition of 5mM HEPES, 1mm NaCl buffer at pH 7.4 at a 50 μM peptide concentration, followed by 2 minutes of vortex. The Aβ(1-42) solution was then filtered with 0.45 μm pore, (Millipore, MILLEX®-HV) and 0.22 μm pore, (Millipore, MILLEX®-GV) filters. For aging experiments, the solution was incubated for the desired time at 37°C. Fluorescent Aβ(1-42) was prepared similarly except that Hilyte Fluor 488-Aβ(1-42)and Aβ(1-42) were initially mixed in HFIP at a 1/1 molar ratio. This fluorescent peptide mixture will be termed Aβ(1-42)* herefrom.

Thioflavin binding measurements

Thioflavin, (Sigma) and Aβ(1-42) were mixed from their stock solutions in 5 mM HEPES, 1mM NaCl buffer at pH 7.4 at final concentrations of 8.8 μM and 5.9 μM respectively. Fluorescence intensity was measured at 37°C in duplicate at excitation and emission wavelength 450 nm and 482 nm respectively.

Dynamic light scattering

Dynamic light scattering, (DLS) of Aβ has been described [39]. A Zetasizer Nano, (Malvern) equipped with a 633 nm He-Ne laser and a 173˚ back-scatter detector was used for DLS measurement. The Aβ(1-42)concentration was 50 μm in 5mM HEPES, 1 mM NaCl buffer at pH 7.4 and the temperature 37°C.

Transmission electron microscopy

Transmission electron microscopy, (TEM) of Aβ was performed as described [40]. For sample preparation, 4 μL of 50 μM Aβ(1-42) solution in 5 mM HEPES, 1mM NaCl buffer at pH 7.4 were deposited on a hydrophilized grid and dried out after 5 minutes with Whatman N˚1 filter paper by capillary effect. 4 μL of 1 % uranyl acetate, (w/v) solution was deposited onto the dried grid. After 30 seconds, the solution was dried with filter paper followed by at least 30 minutes drying at ambient atmosphere.

GUVs Preparation and Fluorescence Microscopy

GUVs were made as described previously [25] by the electroformation method in a temperature-controlled chamber containing 2 mL of HEPES 0.5 mM, pH 7.4, using lipids mixtures containing 0.25 mol % Texas Red PE in diethyl ether/chloroform/methanol 7/2/1 in volume, deposited on platinium electrodes. A Zeiss Axiovert 200 M microscope, (fluorescent unit Fluoarc N HBO 103, Zeiss), equipped with a Lambda 10 unit, (Sutter Instrument Co.), plus a CCD B/W chilled camera, (Cool SNAP HQ), was used for GUV imaging. The setup was computer-controlled by the Metamorph 6.0 software, (Ropper Sci.). A 40× Ph LD Zeiss objective was used. Aβ(1-42)* was added to the GUV chamber at a final concentration of 0.25

μM. For Texas Red and Hilyte Fluor 488 fluorescence, Zeiss filter sets 15, (Ex/Em = 550/620 nm) and 10, (Ex/Em = 470/540 nm) were used respectively. The minimum intensity of the HBO lamp, (25 W) was used.

Large Unilamellar Vesicles Preparation and Spectroscopic Fluorescence Measurements.

LUVs were prepared using the extrusion method as described [41], using HEPES 5 mM, NaCl 1 mM, pH 7.4 buffer. Di-ANEPPS or Laurdan was mixed with the lipids in the initial organic solution at a probe:lipid mole percent of 0.25. and 0.5 mol% respectively. Steady-state fluorescence measurements were carried out with a Cary Eclipse spectrofluorimeter, (Varian Instruments, CA) equipped with a thermostated, (± 0.1°C) cuvette holder. Quartz cuvettes were used. Excitation and emission slits were adjusted to 5 nm. All fluorescence measurements were carried out at a total lipid concentration of 0.2 mM. Samples were equilibrated for 5 min at the desired temperature. Di-ANEPPS fluorescence was excited at 420 nm and 520 nm and detected at 670 nm. Laurdan fluorescence was excited at 355 nm and detected at 440 nm and 490 nm. For kinetics studies, the fluorescence intensity of each sample was initially measured for ca. 10 minutes, then 24 μL of 50 μM of Aβ(1) was added followed by mixing by aged at 37 ˚C for 8 h gentle pipetting. The final peptide/lipid molar ratio was at 1/25. The kinetics was followed for 25 minutes after mixing. It was not followed further due to formations of precipitation especially sphingosine containing sample. Experiments were done at 37 ˚C and 13 ˚C. All fluorescence kinetics experiments were done in triplicate and were consistent within an error range of ± 6%.

RESULTS

1. Characterization of Aβ(1-42) aggregation state.

Our goal in the present study was to investigate whether single chain sphingolipid could modulate membrane binding of Aβ(1-42) in a physiologically relevant manner. The Aβ(1-42) peptide is known to extensively oligomerize and aggregate over time, a property which appears essential in its various roles in the development of AD [42, 43]. Interaction of the peptide with membranes is likely to depend upon its autoassociation state. This raised the issue of which level of Aβ(1-42) aggregation state would be relevant to the present study. Although present in the extracellular medium, Sph and S1P occur mainly intracellularly where enzymes involved in the sphingolipid rheostat are located [23]. Several studies suggest that intracellular Aβ does not occur in the form of fibrils or protofibrils but rather as monomer or oligomers [44]. We therefore chose conditions in which the later species would be favored.

We checked the evolution of Aβ(1-42) over time in our experimental conditions by DLS, TEM and thioflavin binding. It was found that after ca. 9 hours at 37°C, Aβ(1-42) occurred mainly as monomers and oligomers. The results are summarized in Fig. 1 and 2.

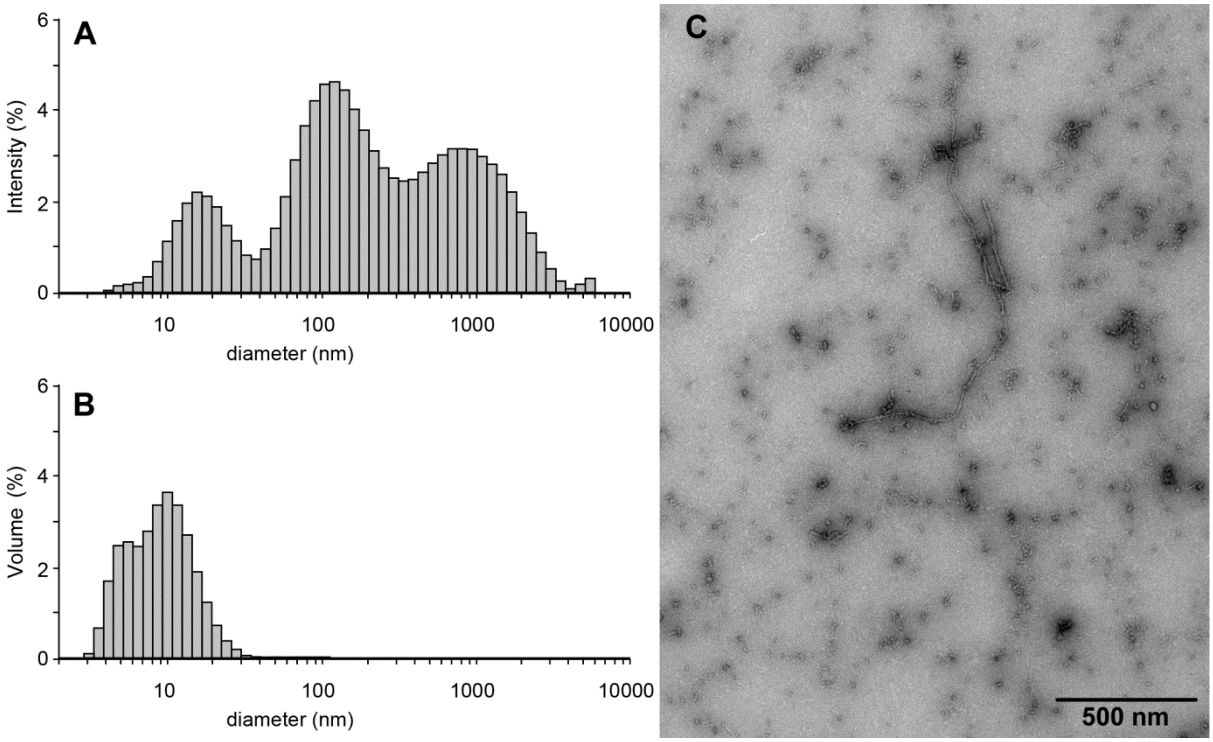

Fig. 1. Aggregation state of 9 hours-aged Aβ(1-42). DLS profiles of ca. 9 hours-aged Aβ Aβ(1-42) plotted in the intensity(A) and volume, (B) representations. TEM of ca. 9 hours-aged Aβ(1-42).

DLS data, plotted using the "intensity" representation, (which overemphasizes higher molecular sizes), points out to the occurrence of 3 types of species with apparent diameters around 14, 50 and 500 nm, (Fig. 1A). The "volume" representation, (which displays species according to their molecular volumic contribution to the sample) indicates that the smaller diameter species is highly majoritary although with a more realistic apparent diameter ranging from 6 to 10 nm, (Fig. 1B). In agreement with previous studies [39], we identify these species as Aβ(1-42) monomers-oligomers, protofibrils and fibrils, monomers-oligomers being in the majority. This is confirmed by TEM which shows a majority of slightly elongated species with dimensions 5 nm together with small amount of larger fibrillar material, (Fig. 1C). The preparation promotes a significant thioflavin fluorescence increase, indicating that the oligomers contain significant β structure, (Fig. 2). Thioflavin T (ThT) binding is a common

method to detect the progression of Aβ aggregation. The dye undergo a large enhancement of its fluorescence emission upon binding to amyloid fibril-type aggregates. Such a drastic change of intensity is due to freezing of the internal rotation of the molecule by binding to the β-sheet structures associated with all amyloid molecular species **[44a]**. We thus chose to perform our membrane interaction studies with ca. 9h-aged Aβ(1-42), since it contains a dominating fraction of Aβ(1-42) oligomers. The zeta-potential of this preparation was performed and found to be -40mV.

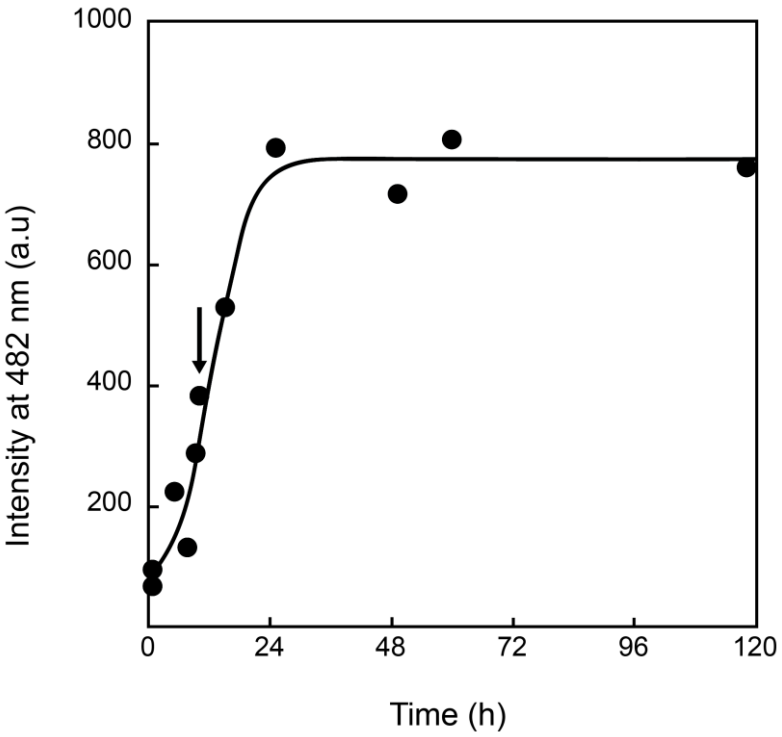

Fig. 2 Thioflavin binding to Aβ(1-42). Thioflavin fluorescence intensity as a function of Aβ(1-42) pre-incubation time at 37°C. The arrow emphasizes the value corresponding to 9 hours-aged Aβ(1-42).

2. Binding of Aβ(1-42) on Sph and S1P-containing GUVs. Influence of phase behavior.

We first investigated the interaction of Aβ(1-42)with EPC GUVs containing Sph or S1P using TR-PE, a lipid probe which partitions in favor of the more fluid regions [45] as well as a fluorescently labeled Aβ(1-42)* preparation, (see Materials and Methods). We have previously studied in detail the lipid phase morphology of such vesicles using TR-PE alone [25]. It was found that EPC/Sph GUVs display Sph-rich gel phase domains with a characteristic flowery shape coexisting with a liquid crystalline phase. These domains melt above a temperature that depends on the Sph content. On the other hand EPC/SP1 vesicles show full miscibility at all studied temperature, (10°C) as a single liquid crystalline phase. Here most of the experiments were performed using double labeling, i.e. withTR-PE-labeled vesicles to which Aβ(1-42)* (aged 9h to favor oligomers), was added directly into the bathing chamber and left to incubate for 20 min before observation. The lipid and peptide-bound fluorescence probes have separated excitation and emission maxima and it was checked with single labeled vesicles that interference of emission of each probe on the other is very limited. In all case it was found that addition of unlabeled or labeled 9 hours-aged Aβ(1-42) does not induce any change of the GUV surface morphology as viewed from TR-PE fluorescence. In particular, the peptide does not induce any change in lipid phase organization. After the addition of Aβ(1-42)* vesicles invariably became fluorescent indicating that the peptide binds to all membranes studied here.

Figure 3A and B shows respectively the TR-PE fluorescence and the Aβ(1-42)* fluorescence of EPC GUVs containing 40% molar Sph at 13°C. The TR-PE fluorescence emphasizes the occurrence of phase separation. Sph-rich gel domains appear as dark flower-shaped regions from which the lipid probe is excluded [25]. Interestingly, the Aβ(1-42)* fluorescence displays a reverse fluorescence pattern, i.e. the flower-shaped gel domains are bright, whereas

the surrounding liquid crystalline phase appears dark. Moreover the boundaries of the domains are significantly more fluorescent than their interior. These data indicate that Aβ(1-42) binds preferentially to the Sph rich gel phase, with a preference to the boundary region, and less to the liquid crystalline phase.

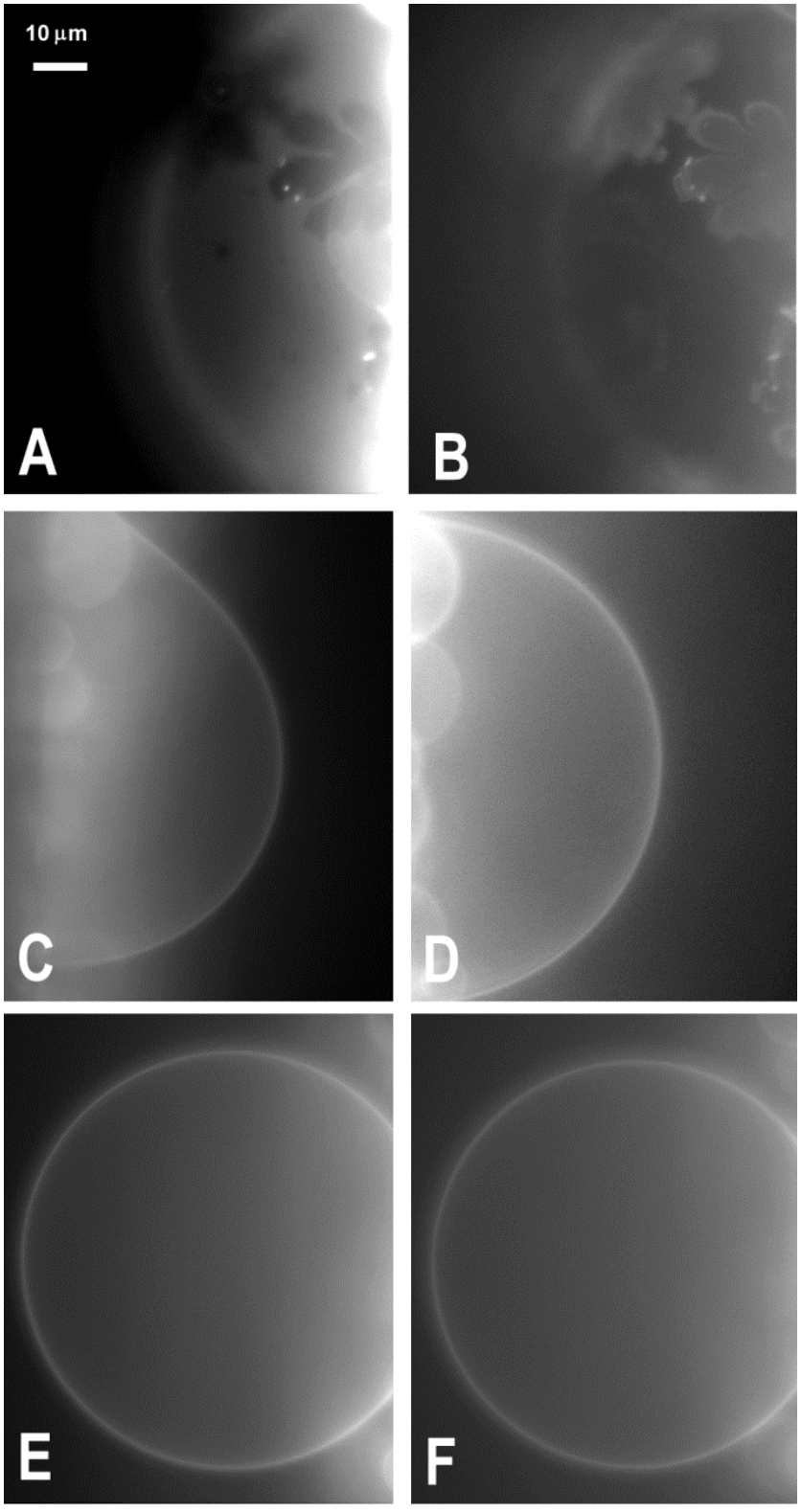

Fig. 3. Phase state behavior and binding of ca. 9 hours-aged Aβ(1-42)* for EPC GUVs labeled with TR-PE and containing single-chain sphingolipids. Fluorescence micrographs of GUVs composed of EPC/Sph 60:40, (mol %) t 13°C, (A, B) and 37°C, (C, D), GUVs composed of EPC/ S1P 60:40, (mol %) at 13°C, (E, F), as visualized by TR-PE, (A, C, E) and Hilyte Fluor, (B, D, F) fluorescence. The data of, (A, B) and, (E, F) was obtained with doubly labeled vesicles. The data of, (C, D) was obtained with 2 singly labeled vesicles.

At 37°C, EPC GUVs containing 40% molar Sph display a homogeneous liquid crystalline phase as reported by TR-PE fluorescence, (Fig. 3C). The Aβ(1-42)* appears to bind evenly to the vesicle surface, (Fig. 3D) as judged from its homogenous fluorescence distribution. In the case of EPC/S1P GUVs, which we reported previously to yield an homogeneous phase at all temperature and sphingolipid content, as shown here for 40% molar S1P and 13°C, (Fig. 3E), Aβ(1-42)* again binds evenly to the vesicle surface, (Fig. 3F).

Thus it appears that Aβ(1-42), binds to GUVs irrespective of composition and temperature. Furthermore, the results indicate a higher affinity for the gel phase and its boundaries and/or Sph.

3. Influence of Sph and S1P on Aβ(1-42) binding to LUVs

We have also studied the binding of Aβ(1-42) to single chain sphingolipid containing model membranes at a more microscopic level. For this we have investigated such binding with LUVs with lipid compositions similar to the above, labeled separately with two distinct lipophilic fluorescence probes, Laurdan and di-8-ANEPPS. Laurdan fluorescence in lipid membranes undergoes a shift in its emission spectrum due to a packing-dependent environmental sensitivity of its excited state relaxation. This is usually expressed as the general polarization $GP = (I_{440}-I_{490})/(I_{440}+I_{490})$ which is a measure of lipid packing at the molecular level [33]. Thus, one has GP = -1 in pure liquid-crystalline, GP = 1 in pure gel phase membrane, and $-1<GP<1$ in any intermediate, (or mixed) membrane states. Therefore, an increase in GP indicates, on average, a more ordered and less hydrated lipid membrane structure.

In the case of di-8- ANEPPS incorporated into LUVs, it has been shown that the fluorescence intensity ratio $R_{ex} = I_{670/exc420} / I_{670/exc520}$ is directly proportional to the dipole potential, independently of fluidity effects [35]. As mentioned in the introduction, the dipole potential is the electrical potential that occurs transversally between the water-lipid interface and the hydrocarbon interior. It is contributed by all polarized and polarizable chemical groups of lipids as well as by water next to and within the bilayer [32]. An increase of R_{ex} corresponds to an increase of membrane dipole potential.

LUVs composed of pure EPC and EPC in the presence of Sph, S1P or both were studied at 13°C and 37°C. The initial GP values decrease with increasing temperature, reflecting an increase in orientational polarizability of the probe environment, hence a decrease in lipid packing, whereas the initial R_{ex} values, hence the dipole potential are hardly modified. Incorporation of Sph, S1P or both in EPC LUVs have specific effects on both packing and dipole potential that have been described previously [25,26].

At 13°C, with both probes and at all lipid composition, addition of Aβ(1-42) to LUVs promoted a relatively rapid, (~5 min) intensity variation without any further evolution in 20 min, (Fig 4, note that there is a 1 min gap without acquisition after Aβ(1-42) addition which corresponds to the sample mixing time.).

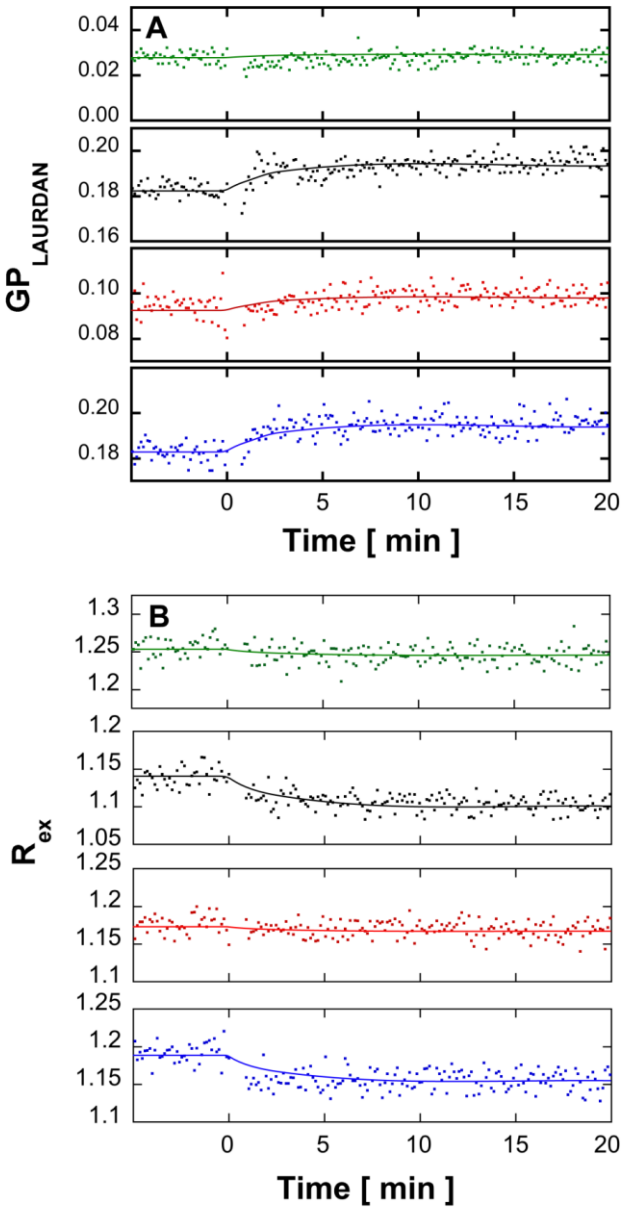

Fig. 4. Effect of Aβ(1-42) on the fluorescence properties of labeled LUVs in the absence or presence of single-chain sphingolipids. Kinetics of variation of Laurdan GP (A) and di-8-ANEPPS R_{ex} (B) after addition of ca. 9 hours-aged Aβ(1-42) to LUVs composed of EPC/Sph/S1P at mole ratios of, from top to bottom, 100:0:0, (green), 60:40:0, (black), 60:0:40, (red) and 60:20:20, (blue) at 13°C. The 1 min gap without acquisition after Aβ addition corresponds to the sample mixing time. Dots correspond to values of GP or Rex calculated from consecutive measurements of the fluorescence emission intensity performed every 15 sec with an averaging time of 1 sec, successively at 440 and 490 nm with excitation at 355 nm for GP and at 670 nm with successive excitations at 420 and 520 nm. All fluorescence kinetics experiments were done in triplicate and were consistent within an error range of ± 6% on the value of the final plateau. The figure shows one representative experiment for each experimental condition.

Fig. 5 shows the maximum variation, (20 min after addition) promoted by Aβ(1-42) on the Laurdan GP values and di-8-ANEPPS R_{ex} values at 13°C. The general trend is an increase of GP, (i.e. decrease in orientational polarizability/increase in packing) and a decrease of $R_{ex,}$ (i.e. decrease of dipole potential). However, at this temperature, these variations appear very small, although significantly higher when Sph is present, (EPC/Sph/S1P 60:40:0 or 60:20:20 mol/mol). This suggests a superficial binding of Aβ(1-42) to membranes at low temperature, which moderately affects orientational polarizability and lipid packing or dipole potential and is slightly enhanced by the presence of Sph, consistently with the higher affinity towards this lipid suggested by the GUVs results. The kinetics data indicates that such superficial membrane adsorption is a fast process, (~5 min).

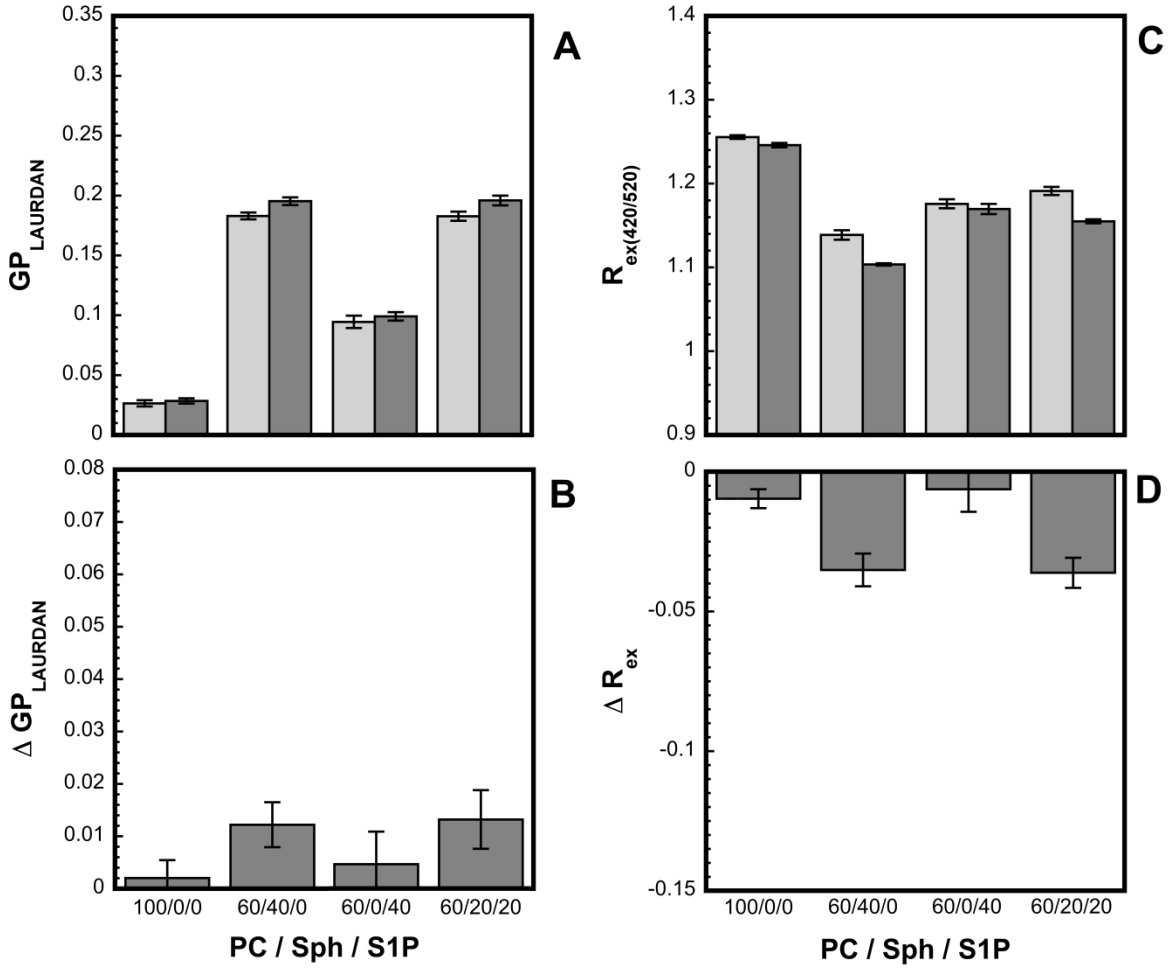

Fig. 5. Effect of Aβ(1-42) on the fluorescence properties of labeled LUVs in the absence or presence of single-chain sphingolipids. Effect of ca. 9 hours-aged Aβ(1-42)binding to LUVs on the Laurdan GP (A, B) and on the di-8-ANEPPS $R_{ex,}$ (C, D) 20 min after peptide addition as a function of the EPC/Sph/S1P mole ratio at 13°C. The total sphingolipid molar percentage is kept constant at 40%(mol/mol). The upper panels, (A, C) correspond to the maximum value of the parameter and the lower panels to its variation after/before Aβ(1-42) addition. Error bars were calculated from the standards deviations associated with the dispersion of the original fluorescence data point within 5 min ranges taken before Aβ(1-42) addition and in the plateau regions. The figure shows the data extracted from one representative fluorescence kinetics experiment for each experimental condition. All fluorescence kinetics experiments were done in triplicate and were consistent within an error range of ± 6%% on the value of the final plateau.

More composition-specific effects were found at 37°C, (Fig. 6). For both probes and with all lipid compositions, addition of Aβ again promoted a relatively rapid, (~5 min) intensity variation. However, in LUVs containing Sph, this rapid phase is followed by a slower phase that reaches a plateau after ca. 15 min. This is particularly visible for EPC/Sph/S1P 60:40:0, (mol/mol) LUVs but also observable to a lesser extent for EPC/Sph/S1P 60:20:20, (mol/mol) LUVs. The occurrence of this slow component was checked by attempting an exponential fit of all kinetics for both probes at both temperatures. Only for Sph-containing LUVs at 37°C was a slow decay rate component significant, (Table I).

Table 1

Decay rate of the slow kinetic component of Laurdan GP and di-8-ANEPPS after addition of 9 hours-aged Aβ(1-42)to Sph-containing LUVs.

Lipid composition **(mol/mol)**	**GP slow component rate** **(s**, mean±SD**)**	**R_{ex} slow component rate** **(s**, mean±SD**)**
EPC/Sph/S1P 60:40:0	0.030 ± 0.005	0.12 ± 0.03
EPC/Sph/S1P 60:20:20	0.027 ± 0.007	0.10 ± 0.06

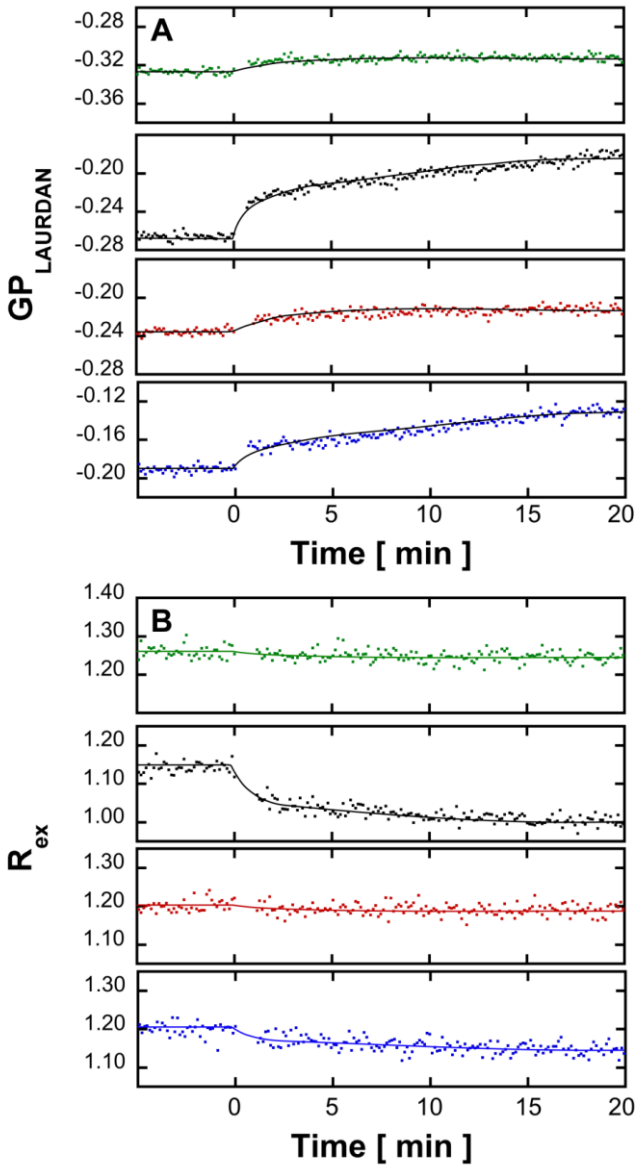

Fig. 6. Effect of Aβ(1-42) on the fluorescence properties of labeled LUVs in the absence or presence of single-chain sphingolipids. Kinetics of variation of Laurdan GP, (A) and di-8-ANEPPS R_{ex} (B) after addition of ca. 9 hours-aged Aβ(1–42) to LUVs composed of EPC/Sph/S1P at mole ratios of, from top to bottom, 100:0:0, (green), 60:40:0, (black), 60:0:40, (red) and 60:20:20 (blue) at 37°C. The 1 min gap without acquisition after Aβ addition corresponds to the sample mixing time. Dots correspond to values of GP or Rex calculated from consecutive measurements of the fluorescence emission intensity performed every 15 sec with an averaging time of 1 sec, successively at 440 and 490 nm with excitation at 355 nm for GP and at 670 nm with successive excitations at 420 and 520 nm. All fluorescence kinetics experiments were done in triplicate and were consistent within an error range of ± 6% on the value of the final plateau. The figure shows one representative experiment for each experimental condition.

Fig. 7 shows the maximum variations, (20 min after addition) promoted by Aβ(1-42) on the Laurdan GP values and di-ANEPPS R_{ex} values at 37°C. In the absence of Sph, (PC, PC/S1P), again small relative changes in GP and R_{ex} are found, indicating again a superficial binding. On the other hand, when Sph is present, (EPC/Sph/S1P 60:40:0 or 60:20:20 mol/mol), larger changes in GP are found, indicating a more significant effect on orientational polarizability and packing, and therefore a stronger interaction of Aβ(1-42) with the membrane. Furthermore, in the case of Sph, Aβ(1-42) binding promotes a much larger change in R_{ex}, and hence of dipole potential. This can be interpreted as resulting from a deeper penetration of Aβ(1-42) in Sph containing membranes in the liquid crystalline state. The biphasic Aβ-induced GP and R_{ex} changes observed with Sph suggest a fast superficial adsorption of the peptide to the membrane, followed by a slow transition towards a state of deeper penetration. Interestingly, when S1P is present with Sph these larger Aβ-induced change in R_{ex} and dipole potential is largely suppressed and the biphasic character of the kinetic is decreased. This suggests that the deeper penetration of Aβ due to Sph is in a large part hindered by S1P which in part, reverses the location of the peptide to more superficial.

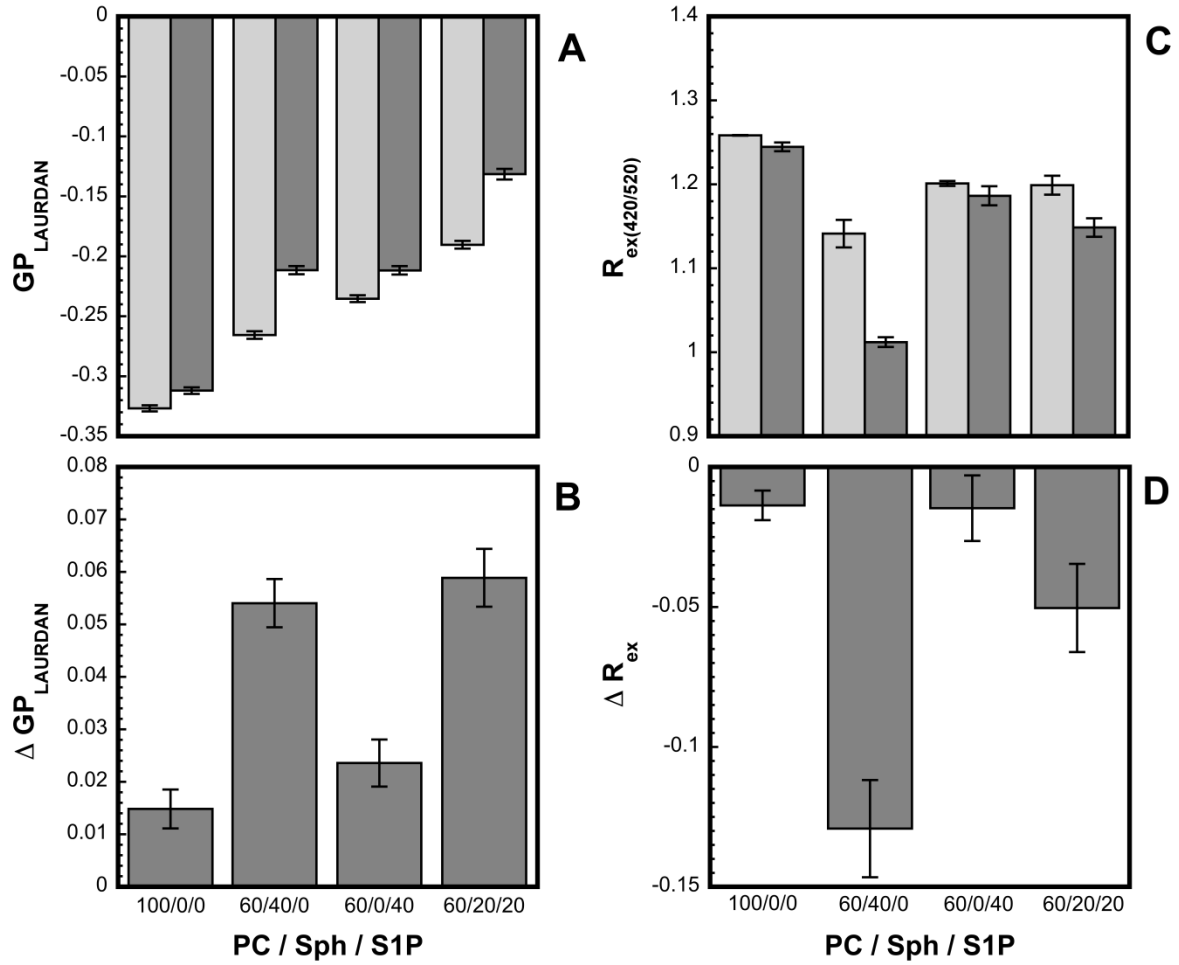

Fig. 7. Effect of Aβ(1-42) on the fluorescence properties of labeled LUVs in the absence or presence of single-chain sphingolipids. Effect of ca. 9 hours-aged Aβ(1) binding to LUVs on the Laurdan GP, (A, B) and on the di-8-ANEPPS $R_{ex,}$ (C, D) 20 min after peptide addition as a function of the EPC/Sph/S1P mole ratio at 37°C. The total sphingolipid molar percentage is kept constant at 40%(mol/mol). The upper panels, (A, C) correspond to the maximum value of the parameter and the lower panels to its variation after/before Aβ(1) addition. Error bars were calculated from the standards deviations associated with the dispersion of the original fluorescence data point within 5 min ranges taken before Aβ(1-42) addition and in the plateau regions. The figure shows the data extracted from one representative fluorescence kinetics experiment for each experimental condition. All fluorescence kinetics experiments were done in triplicate and were consistent within an error range of ± 6%% on the value of the final plateau.

DISCUSSION

In the present study, the effects of the two cell fate effectors sphingolipids Sph and S1P mixed with EPC in model membranes upon Aβ(1−42) oligomer membrane binding were examined using model vesicles. Sph or S1P molar percentages used here ranged from 20 to 40 mol % total lipid whereas overall membrane concentrations of Sph and S1P involved in the sphingolipid rheostat are probably of the order of 1 mol % total lipid [46, 23]. Here the use of such non-physiological concentrations was necessitated by the biophysical techniques used. However, as discussed below, our experiments lead to an interpretation, i.e. the occurence of a selective Aβ(1-42)-sphingosine interaction that could remain valid at low global sphingolipid concentrations if the mutual affinity is high. Whereas, both sphingolipids used in this study are single chain charged lipids that may partition between the lipid phase and water [47-49], in our previous studies, we invariably found important, specific and dose-dependent membrane effects of both compounds either separately or mixed together on zeta-potential, lipid packing, phase behavior and dipole potential that are consistent with quantitative incorporation in the bilayer [25, 26]. Specific and quantatively correlated effects of both sphingolipids were observed in LUVs and GUVs experiments, although the effective lipid concentration is significantly lower in the latter [25]. This suggests that both sphingolipids are mostly located in the membrane in our experiments. This would also rule out the occurrence of an important detergent effect of both single chain sphingolipids in our conditions. In particular in our experience, it would be impossible to form GUVs in the presence of a detergent effect.

In the case of another bioactive lipid, PIP2, the concept of *in situ* high local concentrations at biosynthesis loci and/or inside specific microdomains has been proposed to explain the biological effects [50]. In our previous study, that used similar concentrations of Sph and S1P,

we have invoked similar local concentration arguments [25,26], considering that the enzymes responsible for the biosynthesis of both sphingolipids are located in plasma membrane rafts and that rafts are involved in several of the cellular effects [51-55]. Therefore the local concentrations of effector lipids found in these domains may possibly be of the order of those used in this study. Besides, as confirmed here, it has been found that probably nearly pure Sph gel domains can be formed in model membranes [25,56]. We have proposed that such Sph gel domains may occur *in situ* [25]. Indeed, the cellular occurrence and functional influence of gel domains already appears likely for ceramide, another sphingolipid yielding apoptotic and antiproliferative effects [57, 58]. Thus it appears possible that high local concentrations of single chain sphingolipids occur in cellular membranes and promote or influence the binding of Aβ.

In order to detect and monitor the binding of Aβ(1-42) to GUVs, we made use of a fluorescent Hilyte Fluor 488 Aβ(1-42) in which the fluorophore is covalently linked to the N-ter amide, thereby modifying the charge of the peptide. This peptide has been used several times in cellular and model systems and is considered reasonably similar to Aβ(1-42) [59-62]. Besides in our study, the fluorescent peptide was mixed at a 1/1 ratio with unlabeled peptide. Our studies show that the peptide binds to GUVs whatever the composition. This suggests that lipid composition-related differences found in LUVs with Laurdan and di-ANEPPS are related to the binding mode rather than to the extent of binding.

The two probes used with LUVs provide different information. Laurdan directly reports on orientational polarizability, which depends on local lipid dipolar density and on the degree of freedom of motion the dipole residues in its surroundings. It is generally used to probe lipid packing, i.e. local lipid molecular density in the plane of the membrane, a properties that is affected by any process that locally changes the distance between neighboring phospholipid

molecules in each leaflet/ For peptide binding to a membrane, such events can range from very superficial adsorption through electrostatic interaction to deep penetration. Di-8-ANEPPS provides a measurement of dipole potential, i.e. the electrical potential across each leaflet and therefore probes peptide binding events necessarily involving some penetration. Recent theoretical studies indeed suggest that di-8-ANEPPS possesses a deeper average location in the bilayer than Laurdan [32, 63, 64].

The complementary informations brought by these two probes allow us to distinguish 2 modes of binding of Aβ(1-42) oligomers to membranes, (Fig 8). The first is a superficial binding, obtained with pure EPC, EPC/S1P and EPC/Sph/S1P membranes at 13°C and 37°C as well as with EPC/Sph membranes at low temperature. This mode involves adsorption of the peptide to the membrane that moderately affects lipid packing without much penetration and effect on dipole potential. The second is a deeper binding, observed with EPC/Sph membranes at 37°C, which involves penetration of the peptide inside the bilayer. This binding affects lipid packing (as reflected by orientational polarizability, measured with LAURDAN) more significantly and also affects dipole potential. Kinetic studies suggest that the peptide first rapidly binds superficially to the bilayer then at high temperature in the presence of Sph assumes a deeper positioning.

The superficial binding of Aβ(1–42) to the bilayer likely involves electrostatic interactions of its polar residues with the more superficial lipid headgroup charges. It occurs at the bilayer aqueous interface and minimally perturbs lipid packing (measured as orientational polarizability) and dipole potential. The deeper binding of Aβ(1-42) oligomers to Sph containing bilayers at 37°C probably reflects the combination of an intrinsic affinity of the peptide for this lipid as well as a higher capacity for its bilayer penetration due to the lower packing of the liquid crystalline phase at this temperature. Such affinity is also in part

electrostatic. Our Aβ zeta potential measurement shows that the surface charge of the oligomers is negative, (-40mV). Indeed Aβ(1-42) contains 3 negatively charged residues plus the C-ter. A topographic model of Sph insertion in the bilayer [25] suggests that its amino group is located below the PC phosphate so that the specific interaction with Aβ(1−42) requires penetration of the peptide. Furthermore, the deeper binding may also implicate other parts of the Sph molecule such as the sphingoid backbone. Other effects such as the decrease of the dipole potential provided by Sph may also contribute [26]. Insertion of the peptide itself causes a decrease in dipole potential. Previous results with other peptides mostly also show a decrease of dipole potential [34, 35]. Cladera et al. [35] has emphasized that the contribution of membrane bound peptides to the dipole potential may arise from the direct dipolar contribution of the peptide and from its effect on lipid conformation. Peptide-induced changes in membrane hydration might also contribute. In our previous work [26], it was proposed that the headgroup charged amine of Sph made a significant contribution to the dipole potential observed in the presence of this lipid. Electrostatic interaction of such amino group with Aβ negative groups is therefore likely to affect the dipole potential. Other charges of the peptide might also contribute. In any case, it appears that the deeper positioning of Aβ(1-42) in the bilayer in the presence of Sph is a slower process occuring after an initial rapid superficial binding. Such slow kinetics might be related to lateral diffusion, oligomerization change or transconformation of the peptide. A specific Aβ(1-42)-sphingosine interaction as the origin of the deeper penetration of the peptide appears more likely than an indirect effect of sphingosine on membrane properties. Indeed we have previously found that sphingosine itself (modelately) increases lipid packing, an effect which would rather counteract deeper penetration of a peptide [25].

Our results also show that the concomitant presence of S1P impedes, (although does not completely abolish) the deeper binding of Aβ promoted by Sph. A possible mechanism can be proposed on the basis of our previous work in which we interpreted the synergistic effect of Sph and S1P on lipid packing as resulting from formation of a complex between the two single chain sphingolipids [25]. The involvement of Sph in such a complex would preclude the availability of its amino group for interaction with Aβ(1-42) and therefore the deeper binding, (Fig. 8).

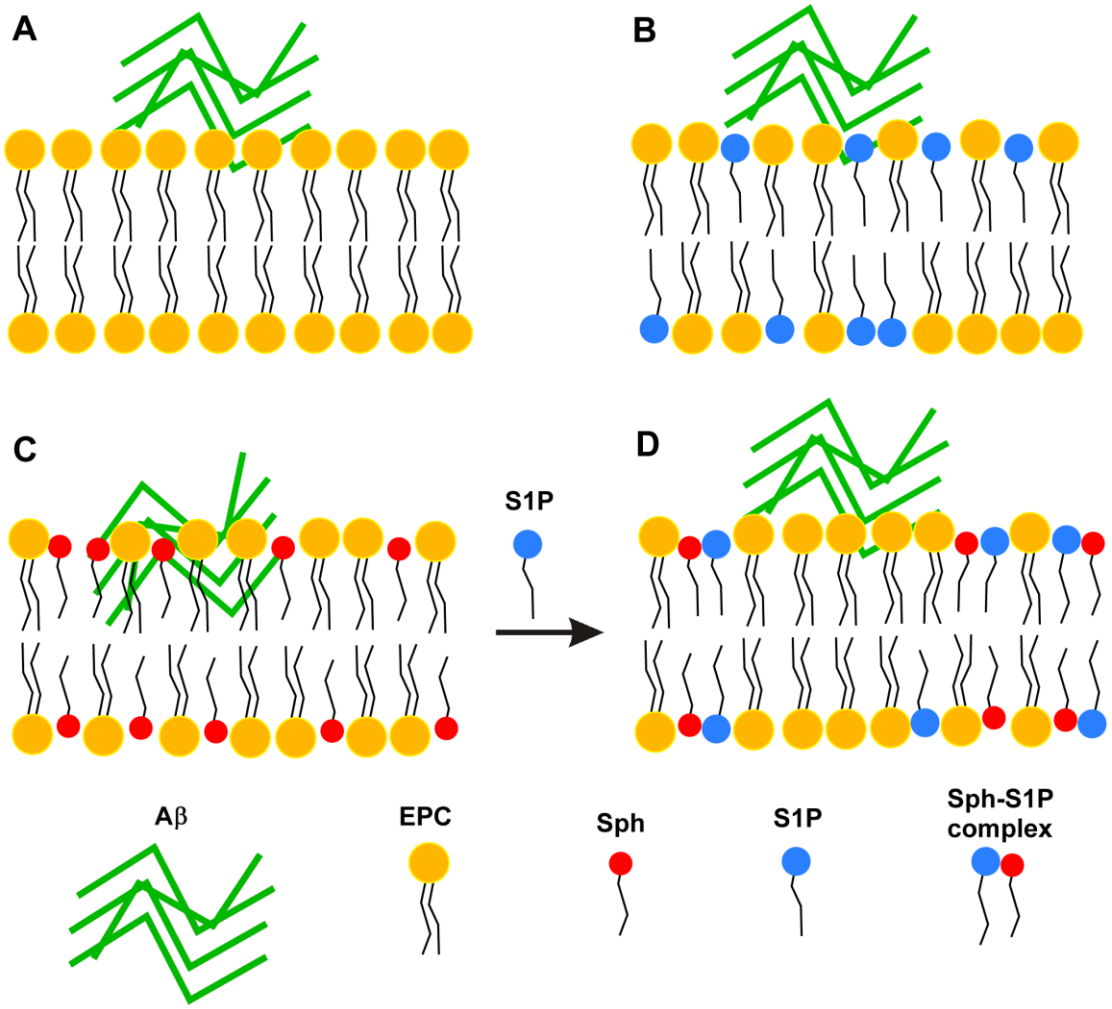

Fig. 8 Schematic drawing of the possible binding modes of Aβ(1-42) to EPC LUVs in the absence or presence of single chain sphingolipids. Superficial binding on EPC bilayers, (A) or in the presence of S1P, (B), deeper binding in the presence of Sph, (C), reversal to superficial binding in the presence of Sph+S1P, (D). The arrow emphasizes the "protecting" effect of S1P upon Sph-induced Aβ(1–42) bilayer penetration

GUV experiments on phase separated membranes also indicate that Aβ(1-42) distinguishes between gel and liquid-cristalline phases. The higher binding of Aβ(1-42) to gel phase in the presence of Sph may reflect an intrinsic affinity of the peptide for this type of phase. However it is more likely a consequence of the preferential interaction of Aβ(1-42) with Sph, although here it is not associated with peptide penetration. Indeed, as emphasized in our previous work [25], the gel phase is likely composed of nearly pure Sph. Thus here the Sph amino group is not embedded into EPC and therefore located at the membrane surface so that Aβ(1–42) negative groups may interact with these without membrane penetration. Besides, it appears that Aβ(1-42) has an even higher affinity for the boundary between gel and liquid-crystalline phase. It is possible that the intrinsically more disordered character of the boundary allows for a tighter interaction with Sph and a deeper penetration of Aβ(1–42) into the bilayer similar to that observed with Sph in the liquid crystalline phase at 37°C. This deeper penetration would not be detectable with spectroscopic methods because of its overall negligible contribution. Other interpretations are possible such as a better accommodation of Aβ(1-42) in the higher curvature interface regions.

It has been highly documented that Aβ(1-42) may have specific interaction with another sphingolipid, GM1, in a cholesterol-modulated manner and occurring possibly in lipid rafts [65, 66]. Since GM1 and Sph have opposite charges, it appears certain that the interaction of Aβ(1–42) with the two lipids is different, involving different conformations of the peptide. However it seems that Aβ(1-42) may have a general affinity for rigid domain either gel or liquid-ordered [17].

The present results may have several consequences with regards to the observed influence of single-chain sphingolipids and the Sph/S1P ratio on the development of AD [27]. Our data suggests that this influence may be related to a selective interaction of oligomeric or

monomeric Aβ(1−42) with Sph that facilitates the development of a pathological mechanism at the intracellular level. This interaction would be relieved by S1P. Besides, since Sph and S1P also occur extracellularly [23] similar processes might occur at the extracellular surface when the peptide is still an extracellular domain of APP, i.e. before cleavage. This might explain the influence of Sph and S1P on the proteolytic release of the peptide [30, 31]. Of course, this does not preclude that the Sph/S1P ratio might influence the development of AD by other mechanisms such as modulation of cell fate-related signaling. Additionally, our study suggests that Aβ(1-42) may have an intrinsic affinity for the boundaries of rigid domains, either gel or raft-type. Nanodomain-microdomain transitions seem to be involved in many signaling processes. Aβ(1-42) may inhibit such processes by binding preferentially to the boundary of nanodomains. This may contribute to the signaling disorders associated with AD [67]. In all, such a study may have direct consequences on the design of chemopreventive and chemotherapeutic dietary lipid approaches for AD.

ACKNOWLEDGEMENTS.

This work was supported by grants from the CNRS, (UMR 7057), the Université Paris-Diderot and the WhoAmI Labex. C.W. acknowledges the support of a Japan Student Services Organization, (JASSO) fellowship. G.S. acknowledges the support of an invited professor grant from the University Paris-Diderot, (Physics Department) as well as the COST Action CM1101-STSM8, during her stay in Paris.

REFERENCES

[1] J. Hardy and D. J. Selkoe, Science 297, (2002) 353.

[2] J. Hardy and D. Allsop, Trends Pharmacol. Sci. 12, (1991) 383.

[3] J. A. Hardy and G. A. Higgins, Science 256, (1992) 184.

[4] V. Nimmrich and U. Ebert, Rev. Neurosci. 20, (2009) 1.

[5] C. Haass and D. J. Selkoe, Nat. Rev. Mol. Cell. Biol. 8, (2007)101.

[6] D. J Selkoe, Behav. Brain Res. 192, (2008) 106.

[7] A. Schmitz, A. Schneider, M. P? Kummer and V? Herzog, Traffic 5, (2004) 89

8] L. M. Billings, S. Oddo, K. N. Green, J. L. McGaugh and F. M. LaFerla, Neuron 45, (2005) 675.

[9] F. M. LaFerla, K. N Green and S. Oddo, Nat Rev Neurosci. 8, (2007) 499.

[10] M. Kaneko, H. Koike, R. Saito, Y. Kitamura, Y. Okuma and Y. Nomura, J Neurosci 30, (2010) 3924.

[11] L. Zheng, A. Cedazo-Minguez, M. Hallbeck, F. Jerhammar, J. Marcusson and A. Terman, Transl. Neurodegener. 1, (2012) 19.

[12] F. G. Sagin and E. Y. Sozmen, Curr. Alzheimer Res. 5, (2008) 4.

[13] I. Morgado and M. Garvey, Adv. Exp. Med. Biol. 855, (2015) 67.

[14] S. Grösgen, M. O. Grimm, P. Friess and T. Hartmann, Biochim. Biophys. Acta 1801, (2010) 966.

[15] L. A. Shobab, G.Y. Hsiung and H. H. Feldman, Lancet Neurol. 4, (2005) 841.

[16] A. Kakio, S. Nishimoto, K. Yanagisawa, Y. Kozutsumi and K. Matsuzaki, Biochemistry 41, (2002) 7385.

[17] M. Vestergaard, T. Hamada, M. Morita and M. Takagi, Curr. Alzheimer Res. 7, (2010) 262.

[18] K. S. Vetrivel and G. Thinakaran, Biochim. Biophys. Acta 1801, (2010)860.

[19] R. Williamson and C. Sutherland, Curr. Alzheimer Res. 8, (2011) 213.

[20] J. Ceccom, M. B. Delisle and O. Cuvillier, Med. Sci. 30, (2014) 493.

[21] G. Van Echten-Deckert, N. Hagen-Euteneuer and I. Karaca, J. Cell. Physiol. Biochem. 34, (2014) 148.

[22] O Cuvillier, Biochim. Biophys. Acta 1585, (2002) 153.

[23] Y. A. Hannun and L. M. Obeid, Nat. Rev. Mol. Cell. Biol. 9, (2008) 139.

[24] H. Fyrst and J. D. Saba, Nature Chem. Biol. 6, (2010) 489.

[25] C. Watanabe, N. Puff, G. Staneva, M. Seigneuret and M. I. Angelova, Langmuir 30, (2014) 139563

[26] C. Watanabe, N. Puff, G. Staneva, M. I. Angelova and M. Seigneuret, Colloids Surf. A 483, (2015) 181.

[27] X. He, Y. Huang, B. Li, C. X. Gong and E. H. Schuchman, Neurobiol. Aging 31, (2010) 398

[28] J. Ceccom, N. Loukh, V. Lauwers-Cances, C. Touriol, Y. Nicaise, C. Gentil, E. Uro-Coste, S. Pitson, C. A. Maurage, C. Duyckaerts, O. Cuvillier and M. B. Delisle, Acta Neuropathol. Commun. 2, (2014) 12

[29] T. A. Couttas, N. Kain, B. Daniels, X. Y. Lim, C. Shepherd, J. Kril, R. Pickford, H. Li, B. Garner and A. S. Don, Acta Neuropathol. Commun. 2, (2014) 9.

[30] N. Takasugi, T. Sasaki, K. Suzuki, S. Osawa, H. Isshiki, Y. Hori, N. Shimada, T. Higo, S. Yokoshima, T. Fukuyama, V. M. Lee, J. Q. Trojanowski, T. Tomita and T. Iwatsubo, J. Neurosci. 31, (2011) 6850.

[31] I. Karaca, I. Y. Tamboli, K. Glebov, J. Richter, L. H. Fell, M. O. Grimm, V. J. Haupenthal, T. Hartmann, M. H. Gräler, G. van Echten-Deckert and J. Walter, J. Biol. Chem. 289, (2014) 167612.

[32] G. Parisio, A. Marini, A. Biancardi, A. Ferrarini and B. Mennucci, J. Phys. Chem. B. 115, (2011) 9980.

[33] T. Parasassi, G. De Stasio, G. Ravagnan, R. M Rusch, and E. Gratton, Biophys. J. 60 (1991) 179.

[34] R. J. Clarke, Adv. Colloid Interface Sci. 89, (2001) 263.

[35] R. J. Clarke and D. J. Kane, Biochim. Biophys. Acta. 1323, (1997) 223.

[36] R. J. Clarke, Biophys. J.. 109, (2015) 1513.

[37] J. L. Richens, J. S Lane, J. P. Bramble and P. O'Shea, Biochim. Biophys. Acta 1848, (2015) 1828.

[38] J. Cladera, I. Martin, J. M. Ruysschaert, P. O'Shea, J. Biol. Chem. 274, (1999) 299519.

[39] P. Cizas, R. Budvytyte, R. Morkuniene, R. Moldovan, M. Broccio, M. Lösche, G. Niaura, G. Valincius and V. Borutaite, Arch. Biochem. Biophys. 496, (2010) 84.

[40] V. L Anderson, T. F. Ramlall, C. C. Rospigliosi, W. W. Webb and D. Eliezer, Proc. Natl. Acad. Sci. USA, 107, (2010) 188505.

[41] N. Khalifat, J. B. Fournier, M. I. Angelova and N. Puff, Biochim. Biophys. Acta. 1808, (2011) 2724.

[42] L. C. Serpell, Biochim. Biophys. Acta 1502, (2000) 16.

[43] C. G. Glabe, J. Biol. Chem. 283, (2008) 296393.

[44] M. Sakono and T. Zako, FEBS J. 277, (2010) 1348.

[44a] M. Biancalana and S. Koide, Biochim. Biophys. Acta, 1804, (2010) 1405.

[45] L. A. Bagatolli, Biochim. Biophys. Acta. 1758, (2006) 1541.

[46] Y. Yatomi and Y. Higarashi, Acta Biochim. Polonica 45, (1998)299.

[47] H. Sasaki, H. Arai, M. J. Cocco, and S. H. White, Biophys. J. 96 (2009) 2727.

[48] F. X. Contreras, J. Sot, A. Alonso and F. M. Goñi, Biophys. J. 90 (2006) 4085.

[49] M. García-Pacios, M.I. Collado, J. V Busto, J. Sot, A. Alonso, J.-L.R. Arrondo and F. M. Goñi, Biophys. J. 97 (2009) 1398.

[50] D. W. Hilgemann, Pflugers Arch. Eur. J. Physio.l 45, (2007) 55.

[51] N Augé, M Nikolova-Karakashian, S Carpentier, S Parthasarathy, A Nègre-Salvayre, R Salvayre, AH Merrill Jr and T Levade, J. Biol. Chem. 274, (1999) 215338.

[52] A. Olivera. and S.. Spiegel, Nature 365, (1993) 557.

[53] J. A. Hengst, J. M. Guilford, T. E. Fox, X. Wang, E. J. Conroy and J. K. Yun, Arch. Biochem. Biophys. 492, (2009) 62.

[54] J. M. Ryu, Y. B Baek, M. S Shin, J. H. Park, S. H. Park, J. H. Lee and H. J. Han, Stem Cell Res. 12, (2014) 69.

[55] J. Zhao, P. A. Singleton, M. E. Brown, S. M. Dudek and J. G. Garcia, Cell Signal 21, (2009) 1945.

[56] R. Georgieva, K. Koumanov, A. Momchilova, C. Tessier and G. Staneva. J.. Colloid Interf. Sci. 350, (2009)502.

[57] B. Stancevic and R. Kolesnick, FEBS Lett. 584, (2010) 1728.

[58] Y. Zhang, X. Li, K. A. Becker. and E. Gulbins, Biochim. Biophys. Acta 1788, (2009) 178.

[59] A. Halle, V. Hornung, G. C. Petzold, C. R. Stewart, B. G. Monks, T. Reinheckel, K. A. Fitzgerald, E Latz, KJ Moore and DT Golenbock, Nature Immunol. 9, (2008)857.

[60] S. E. Hickman, E. K. Allison and J. El Khoury, J. Neurosci. 28, (2008)8354.

[61] P. Chakrabarty, K. Jansen-West, A. Beccard, C. Ceballos-Diaz, Y. Levites, C. Verbeeck, A. C. Zubair, D. Dickson, T. E. Golde and P. Das, FASEB J. 24, (2010) 548.

[62] E. K. Esbjörner, F. Chan, E. Rees, M. Erdelyi, L. M. Luheshi, C. W. Bertoncini, C. F. Kaminski, C. M. Dobson and G. S. Kaminski Schierle, Chem. Biol. 21, (2014) 732.

[63] D. Robinson, N. A. Besley, P. O'Shea and J. D. Hirst, J. Phys. Chem. B. 115, (2011) 4160.

[64] J. Barucha-Kraszewska, S. Kraszewski and C. Ramseyer, Langmuir. 29, (2013) 1174.

[65] K. Yanagisawa, Biochim. Biophys. Acta 1768, (2007) 1943.

[66] K. Matsuzaki, Acc. Chem. Res. 47, (2014) 2397.

[67] J. A. Godoy, J. A. Rios, J. M. Zolezzi, N. Braidy and N. C. Inestrosa, Cell Commun. Signal .12, (2014) 23.